

DYNAMIC WETTING AND DEWETTING: COMPARISON OF EXPERIMENT WITH THEORIES

Evgeniya.G. Orlova^{1,*}, *Ekaterina R. Malyhina*¹, *Dmitriy.V. Feoktistov*¹, and *Larisa.S. Zhidkova*¹

¹National Research Tomsk Polytechnic University, 634050 Tomsk, Russia

Abstract. The dynamics wetting/dewetting of a metal surface by distilled water drop was studied experimentally. The advancing and receding dynamic contact angles were obtained as a function of a contact line speed. The hydrodynamic and molecular-kinetic models have been applied to the experimental data to interpret the obtained results. The independent variables of the molecular-kinetic and hydrodynamic models, and the determination coefficient were determined by fitting procedure. The receding contact angles are found to be fitted better to the wetting models in comparison with the advancing dynamic contact angles.

1 Introduction

Technological processes of spray cooling, cultivated crop dusting, spin soldering, spray coating, DNA synthesis are based on the drop spreading and evaporation phenomena [1-7].

When the liquid is moving over the solid substrate, a dynamic contact angle (DCA) is established. This angle reflects the balance between driving and drag forces and is a function of a three-phase contact line (CL) speed.

To describe the physical process of spreading, several theories predicting the relationship between the DCA and the CL speed were developed. These theories can be classified according to the mechanisms of energy dissipation in the vicinity of the contact line: molecular-kinetic (MKT) [8, 9] and hydrodynamic [10, 11] theories.

The molecular kinetic theory considers the molecular jumps at the CL as a rate-activated, with an equilibrium frequency k_0 and a displacement distance λ . So, the relationship between the DCA θ_D and the CL speed U is described by [8]:

$$\theta_D = \arccos \left[\cos \theta_s - \left(\frac{2k_B T}{\sigma_{LV} \lambda^2} \right) \arcsin \left(\frac{U}{2k_0 \lambda} \right) \right] \quad (1)$$

where k_B is the Boltzmann constant, T the liquid temperature, θ_s the static contact angle, and λ and k_0 are parameters corresponding to the length of displacement and frequency constant for molecular displacements of the contact line.

* Corresponding author: lafleur@tpu.ru

Nowadays, there is no definitive way of predicting the constants λ and k_0 apriori for a given solid/liquid system. For this reason, these parameters are usually obtained from experiment by curve fitting procedures [12]. The experimentally determined parameters obtained by different scientific groups are listed in Table 1.

Table 1. Fitting parameters of molecular-kinetic model obtained in some works.

Reference	Liquid	$\theta_s, ^\circ$	λ, nm	k^0, Hz
[13]	water	-	0.3	$2 \cdot 10^{10}$
[14]	water	82	0.36	$8.6 \cdot 10^9$
[15]	water	54.1	1.02	$1.19 \cdot 10^3$
[16]	water	55.5	1.79	$6.67 \cdot 10^5$
[17]	glycerine solution	-	7.3	$3.4 \cdot 10^7$

According to the hydrodynamic model the moving process of the contact line is dominated by the viscous dissipation of the liquid; and the bulk viscous friction is the main resistance force for the contact line motion. The shear flow in the vicinity of the contact line leads to a viscous bending of the liquid/vapor interface. For this reason, the dynamic contact angle deviates from its equilibrium value, and can be defined as [10]:

$$\theta_D^3 = \theta_s^3 \pm \left(\frac{9\mu U}{\sigma_{LV}} \right) \ln \left(\frac{L}{L_m} \right) \quad (2)$$

where L is a characteristic capillary length, and L_m the slip length. In Eq. (2) the plus sign applies to the advancing liquid movement and the minus sign applies to the receding liquid movement.

The capillary length is given by [18]:

$$L = \sqrt{\frac{2\sigma_{LV}}{\rho g}} \quad (3)$$

where σ_{LV} is surface tension at the liquid/vapour interface, and ρ the liquid density.

The slip length L_m is the fitting parameter. It represents the length of the region where the no-slip boundary condition of classical continuum theory does not hold, so this value should be in the order of molecular dimension [15].

The aim of this work is to obtain the dependences of the advancing and receding dynamic contact angles from the contact line speed of a drop when it spreads over the metal surface. Also the reconciliation of experimental data with the hydrodynamic and molecular-kinetic models of wetting dynamics was undertaken.

2 Materials and methods

Experimental setup (fig.1) was used to study the wetting and spreading over the solid substrate [19, 20].

Experimental setup consists of the electronic syringe pump 1 to supply the distilled water through the opening 2 mm in diameter from the lower side of the substrate 2. Thus, the bottom-up method [21] for drop formation (0.3 ml) with a liquid flow rate of 0.04 ml/s was implemented. The substrate was set on the special platform, which can be heated from the bottom side of the thermoelectric module 3 attached to the aluminium plate of the goniometer 4. To record the temperature, the chromel-alumel thermocouples 5 were used.

The light beam from the source 8 passed through a fiber-optic illuminator, and converted to the plane-parallel light. The drop spreading over the surface was lighted, and the shadow images of this process were obtained by the high-speed camera Fastvideo-500M (with a maximum resolution of 1280×1024 pixels and at 10 frames per second) equipped with a macro lens.

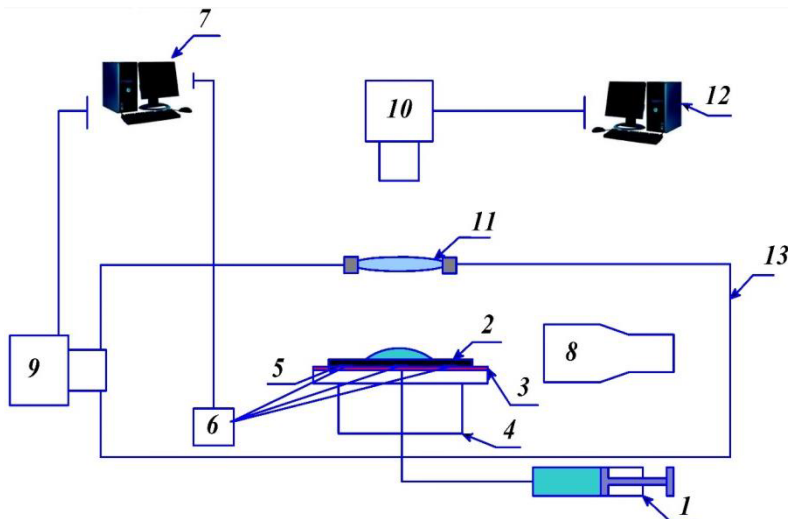


Fig. 1. The scheme of the experimental setup: 1 – syringe pump; 2 – substrate; 3 – thermoelectric module; 4 – goniometer; 5 – thermocouples; 6 – analog-to-digital converter; 7, 12 – personal computers; 8 – light source; 9, 10 – high-speed video cameras; 11 – lens of the upper optical system; 13 – transparent box.

Control of the geometrical shape of the drop was carried out by the high-speed camera 10. To increase the size of the video frames, the lens 11 was used.

The experimental setup is isolated from the external factors changing the temperature, velocity of air flows and environmental humidity by the transparent box 13 made of polymer glass with 3 mm thick.

The substrate made of brass was used in the experiment. Its surface was studied by profilometer “Micro Measure 3D station”. The arithmetic average surface roughness for the brass substrate is equal to 0.016 μm .

The error of dosing by the syringe pump does not exceed 2%. Random error is calculated from the results of repeated experiments. To do this, from two to six experiments were performed at fixed values of the studied factors. Thereafter, the mean values of the contact angle and standard deviations were defined. The variation coefficients were equal to from 10% to 14%. Random errors of measurements were mainly due to the small limits when dispensing liquid through a silicone tube.

3 Results and discussion

According to results of the experiments the advancing and receding DCA were defined during wetting and dewetting of the substrate. The spreading of the drop starts at contact angle of $83.6^\circ \pm 1.5^\circ$ that corresponds to the maximal CL speed (1.76 mm/s). The spreading ends at the angle of $72.1^\circ \pm 1.5^\circ$. This value corresponds to the the pre-measured static angle of water/brass/air system $\theta_s = 70.8 \pm 1.5^\circ$. The CL speed in this case is equal to zero.

Then the drop relaxes [13], and the dewetting starts. The liquid is being withdrawn by the syringe pump, and the receding DCA is being formed.

The hysteresis of the contact angle is defined as the difference between the advancing and receding DCA, when the CL speed is equal to zero (fig. 2).

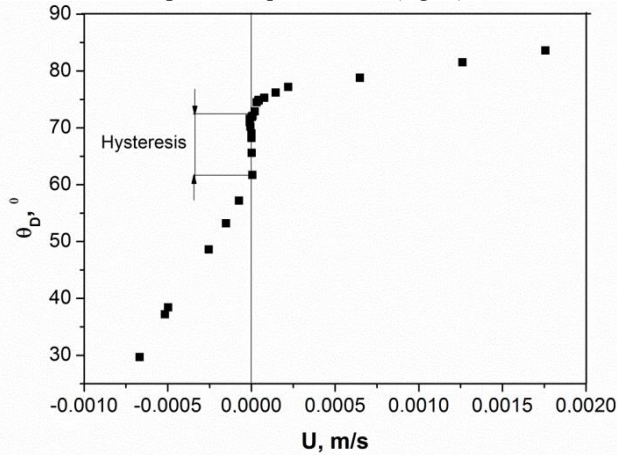


Fig. 2. The advancing and receding dynamic contact angles versus contact line speed. The contact angle hysteresis.

The equations of MKT (1) and hydrodynamic models were used for interpretation of the experimental data and obtaining of functional dependences of the DCA from the CL speed.

Figure 3 shows the dependences of the advancing and receding DCA from the CL speed.

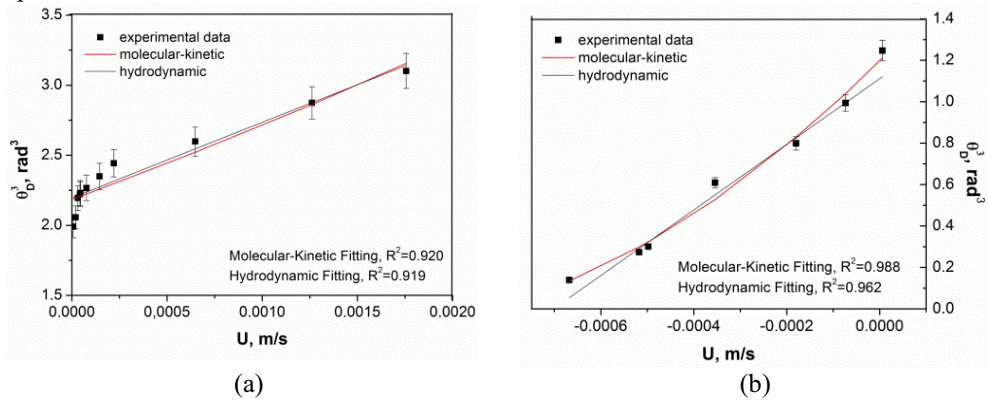


Fig. 3. Fitting of the MKT and hydrodynamic models to (a) the advancing DCA and (b) the receding DCA.

The treatment of the experimental data was performed by the least squares method. After that, the obtained experimental data of advancing and receding DCA have been separately fitted to the MKT and hydrodynamic wetting models. To estimate the reconciliation of the experiment and models, determination coefficient R^2 has been obtained (fig. 3).

According to the results of the reconciliation with the molecular-kinetic model two independent variables were defined: the length of displacement and frequency constant for molecular displacements of the contact line. An initial guess input of k^0 и λ were taken from Table 1.

The value of the $\ln\left(\frac{L}{L_m}\right)$ parameter was determined at fitting the experimental data with the hydrodynamic model. The value of the L_m parameter are not presented separately, because it is not physically meaningful. Probably, this is due to the fact that the value of the capillary number $Ca = \frac{\mu U}{\sigma_{LV}}$ in Eq. (2) is smaller, in order of 10^{-6} for distilled water, in comparison with the value of θ_s^3 .

The values of the molecular-kinetic and hydrodynamic parameters and R^2 values from the fitting for the advancing and receding contact line are listed in Table 2.

Table 2. Fitting parameters of molecular-kinetic and hydrodynamic models obtained in work.

	$\theta_s, ^\circ$ (measured)	Molecular-kinetic model				Hydrodynamic model		
		$\theta_s, ^\circ$	$K^0, 10^9 \text{ Hz}$	$\lambda, \text{ nm}$	R^2	$\theta_s, ^\circ$	$\ln\left(\frac{L}{L_m}\right)$	R^2
Advancing CL	$70.8 \pm 1.5^\circ$	74.4	8.13	0.042	0.920	62.6	44400	0.919
Receding CL		60.9	6.51	0.025	0.988	58	12700	0.962

It was found that Eq. (1) and (2) fit well with the experimental data. However the receding contact angles $\theta_R = f(U)$ were fitted better in comparison with the advancing DCA $\theta_A = f(U)$. It is confirmed by the values of the determination coefficients for the receding contact line $R^2=0.988$ and $R^2=0.962$ for the molecular-kinetic and hydrodynamic models, respectively.

Acknowledgments

The reported study was supported by the grant of President of Russian Federation for the government support of young Russian scientists (MK-6810.2016.8).

References

1. W.M. Grissom, F.A. Wierum, Int J Heat Mass Transf. **24**, 261 (1981)
2. D.V. Zaitsev, O.A. Kabov, Microgravity Sci Technol. **19**, 174 (2007)
3. D.O. Glushkov, G.V. Kuznetsov, P.A. Strizhak, R.S. Volkov, Thermal Science **20**, 131 (2016)
4. D.V. Zaitsev, E.A. Chinnov, O.A. Kabov, I.V. Marchuk, Technical Physics Letters **30**, 231 (2004)
5. V.P. Lebedev, V.V. Lemanov, S.Ya. Misyura, V.I. Terekhov, Fluid Dynamics **28**, 624 (1993)
6. S.Ya. Misyura, International Journal of Heat and Mass Transfer **71**, 197 (2014)
7. K. Batischeva, E. Orlova, D. Feoktistov, EPJ Web Conf. **19**, 01001 (2014)
8. T. D. Blake, J. M. Haynes, J. Colloid Interface Sci. **30**, 421 (1969)
9. E. Ruckenstein, C. S. Dunn, J. Colloid Interface Sci. **59**, 135 (1977)
10. R. G. Cox, J. Fluid Mech. **168**, 169 (1986)
11. O. V. Voinov, J Fluid Dyn **11**, 714 (1976)

12. T.D. Blake, *J Colloid Interf Sci* **299**, 1 (2006)
13. R. Sedev, *Adv Colloid Interface Sci.* **222**, 661 (2015)
14. T.D. Blake, M. Bracke, Y.D. Shikhmurzaev, *Phys. Fluid* **11**, 1995 (1999)
15. S.R. Ranabothu, C. Karnezis, L.L. Dai, *J. Colloid Interf. Sci.* **288**, 213 (2005)
16. R. Fetzer, J. Ralston, *J. Phys. Chem. C.* **113**, 8888 (2009)
17. J.-H. Kim, H.P. Kavehpour, J.P. Rothstein, *Phys. Fluids* **27**, 032107 (2015)
18. M. Schneemilch, R. A. Hayes, J. G. Petrov, J. Ralston, *Langmuir* **14**, 7047 (1998)
19. E.G. Orlova, G. V. Kuznetsov, D. V. Feoktistov, *EPJ Web Conf.* **82**, 01053 (2015)
20. D. Feoktistov, E. Orlova, A. Islamova, *EPJ Web Conf.* **110**, 01018 (2016)
21. K. Gleason, S.A. Putnam, *Langmuir* **30**, 10548 (2014)